Hardware Design and Testing of SUPERball,
a Modular Tensegrity Robot

Andrew P. Sabelhaus[1,*], Jonathan Bruce[2,*], Ken Caluwaerts[3,*], Yangxin Chen[4], Dizhou Lu[5],
Yuejia Liu[6], Adrian K. Agogino[7,*],Vytas SunSpiral[8,*], Alice M. Agogino[9]

I. Abstract

We are developing a system of modular, autonomous "tensegrity end-caps" to enable the rapid exploration of untethered tensegrity robot morphologies and functions. By adopting a self-contained modular approach, different end-caps with various capabilities (such as peak torques, or motor speeds), can be easily combined into new tensegrity robots composed of rods, cables, and actuators of different scale (such as in length, mass, peak loads, etc). As a first step in developing this concept, we are in the process of designing and testing the end-caps for SUPERball (Spherical Underactuated Planetary Exploration Robot), a project at the Dynamic Tensegrity Robotics Lab (DTRL) within NASA Ames's Intelligent Robotics Group. This work discusses the evolving design concepts and test results that have gone into the structural, mechanical, and sensing aspects of SUPERball. This representative tensegrity end-cap design supports robust and repeatable untethered mobility tests of the SUPERball, while providing high force, high displacement actuation, with a low-friction, compliant cabling system.

II. Introduction

Tensegrity robots are inherently compliant, like biological structures, and globally distribute forces within the structure. Thus tensegrity robots are well suited for physical interactions with complex and poorly modeled natural environments. Tensegrity structures also have a high strength-to-weight ratio which is attractive for planetary exploration missions due to the potential to lower launch mass and reduce overall mission cost. It has been shown that large tensegrity structures can be deployed from small compact configurations which enable them to fit into space-constrained launch fairings [1]. The Dynamic Tensegrity Robotics Lab (DTRL) at the NASA Ames Research Center seeks to exploit this inherent compliance, along with the unique force distribution qualities of tensegrity structures, for the next-generation rovers utilized in planetary exploration missions.

The SUPERball (Spherical Underactuated Planetary Exploration Robot) project seeks to develop a tensegrity robotic probe with an actively controllable tensile network that can be compactly stowed for launch, deployed in preparation for landing, land with little or no extra equipment, protect a payload of scientific instruments much like an airbag, and

Fig. 1. SUPERball, Spherical Underactuated Planetary Exploration Robot Ball. Left: v1.5 end-cap Assembly Prototype. Right: Render of full robot.

then achieve dynamic locomotion over unknown terrain [1]. SUPERball will combine Entry, Descent and Landing (EDL) with ground locomotion in a single robotic system. Work has focused on a 6-strut icosahedron for simplicity of design, since this is the lowest-order tensegrity system in a symmetric spherical shape that would tend toward rolling locomotion. The knowledge that there are many other morphologies to be explored as SUPERball matures from a fundamental research project supported by the NASA Innovative Advanced Concepts (NIAC) program, towards a potential future mission has inspired the modular approach that will enable heterogeneous end-caps to be assembled into a wide range of novel tensegrity structures.
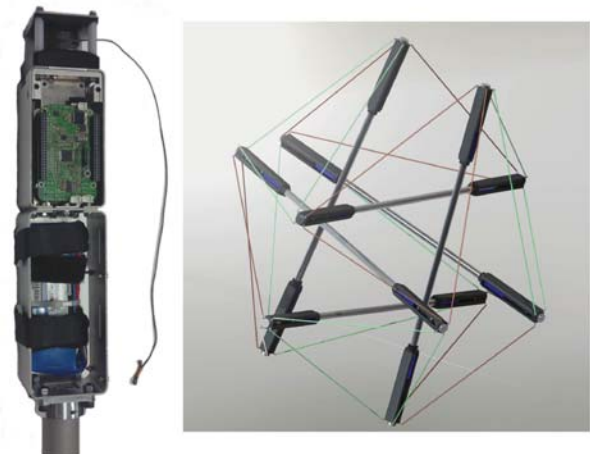
[1]Andrew P. Sabelhaus is with the Dept. of Mechanical Engineering, University of California Berkeley, USA. apsabelhaus@berkeley.edu
[2]Jonathan Bruce is with the USRA/University of California Santa Cruz, USA. jbruce@soe.ucsc.edu
[3]Ken Caluwaerts is with the Electronics and Information Systems Department, Ghent University, Belgium. ken.caluwaerts@ugent.be
[4]Yangxin Chen is with the Department of Mechanical Engineering, University of California Berkeley, USA. okingjo@berkeley.edu
[5]Dizhou Lu is with the Department of Mechanical Engineering, University of California Berkeley, USA. ludizhou@berkeley.edu
[6]Yuejia Liu is with the Department of Mechanical Engineering, University of California Berkeley, USA. yuejialiu@berkeley.edu
[7]Adrian K. Agogino is with UARC/University of California, Santa Cruz, USA. adrian.k.agogino@nasa.gov
[7]Vytas SunSpiral is with SGT Inc., USA. vytas.sunspiral@nasa.gov
[8]Alice M. Agogino is with the Department of Mechanical Engineering, University of California Berkeley, USA. agogino@berkeley.edu
[*]Authors associated with the NASA Ames Research Center - Intelligent Robotics Group, Moffett Field, USA.

III. Background and Previous Work

Although the extensive bio-inspiration surrounding tensegrity systems is a motivating factor for their use as robots [2], many challenges need to be addressed in the practical design and engineering of such robots. Tensegrity systems are highly non-linear, structurally compliant, and dissipate forces globally, which places these systems outside the design space and engineering tools of traditional robotics engineering. Key challenges include open questions on best practices for modularity, actuator type/placement, sensor design/placement, closed loop control, system engineering, power systems, and communication. To date, the majority of constructed tensegrity robots have been designed for open loop control, utilizing servo motors and limited sensing, and are often tethered for power and control [3], or have been secured to the ground [4] [5]. Some related approaches utilize tensegrities as part of a larger, more complicated system, but not as the primary locomotion method [6]. Others have created designs that do not use direct cable actuation, but instead produce forms of locomotion through structural vibration [7] [8]. Our approach to modular end-cap design builds upon earlier prototypes [9] [10] [11] by strictly avoiding any tethering or cable connections between rods, providing the onboard sensing and embedded computing required for true distributed controls, and providing high-strength actuation to enable the completed robot to carry significant extra mass, such as payloads of scientific instruments.

Fig. 2. The ReCTeR prototype next to a single rod of SUPERball, two designs of 6-bar tensegrity robots.

SUPERball, and its predecessor, ReCTeR, are tensegrity robotic systems with 6 structural rods which form an icosahedral geometric shape when all cables are equal length [12]. ReCTeR has 6 motors distributed equally between 3 of the 6 structural rods, while SUPERball has 12 motors, one in each end-cap. A unique feature of ReCTeR is that its main 24 structural cables, which define the traditional icosahedral form, are passive and the 6 additional actuated cables cross the interior of the structure, providing greater force generation when rolling. The modular end-caps designed for SUPERball enable structural experimentation, and have cable mounting brackets such that the actuated cables and passive cables can be assembled in a variety of ways. Thus, using these end-caps, SUPERball can be assembled such that the 12 actuated cables are part of the 24 structural cables, or extra passive cables can be added and the actuated cables connected along internal transects as done for ReCTeR.

Each rod in SUPERball consists of three main elements: two modular end-cap assemblies containing all the mechanical and electrical systems, and a connecting strut tube as a support structure. Each end-cap is independent and can be removed from the connecting rod as one whole unit and is capable of closed loop actuation of one cable. Figure 2 shows both ReCTeR and a single rod from the first iteration of SUPERball. Initial exploration of designs for a second end-cap with similar requirements and capable of closed-loop control of two cables per end-cap are reported in [13].

In parallel to developing modular end-caps for the rapid exploration of hardware prototypes, the DTRL team at NASA Ames is developing the NASA Tensegrity Robotics Toolkit (NTRT) to enable the rapid exploration of structural morphologies and control strategies in a simulated physics based environment [14]. NTRT has recently been approved for release as an Open Source software project[1]. NTRT is designed as a library that runs on top of the Bullet Physics Engine, which is an open source discrete time physics simulator [15]. NTRT provides builder tools for the rapid creation of novel tensegrity structures and tools for design of controllers and parameter learning. Bullet calculates rigid body contact dynamics in real time, though its default soft-body dynamics lack realistic

TABLE I

Original SUPERball Engineering Design Requirements.

Parameter	Value
Mass Per Rod	1.5kg
Maximum Actuator Speed	0.6m/s
Maximum Cable Force	100N
Maximum Compression force	800N

material properties and do not provide engineering level analysis for elastic materials such as cables and springs. Thus, NTRT provides accurate models of cable and spring dynamics, which were validated against hardware prototypes [16]. In combination with other tools to analyze stiffness and load responses when landing, we used NTRT to study dynamic interactions with the environment during locomotion such that engineering design requirements for SUPERball could be obtained through an iterative process utilizing the simulator and machine learning of control algorithms. The designs below were driven by these high-level performance requirements in Table I.
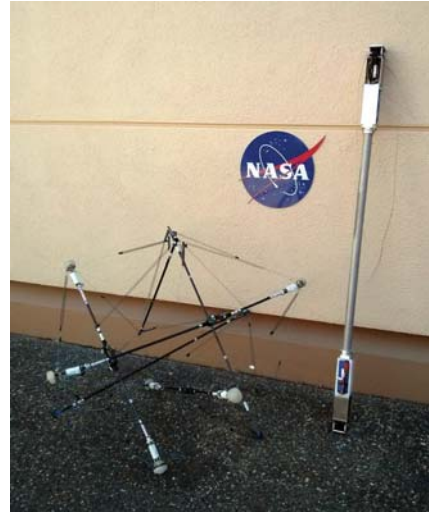
[1]http://ti.arc.nasa.gov/tech/asr/intelligent-robotics/tensegrity/ntrt/

IV. SUPERball Detailed Design

The initial design concept for SUPERball was published Bruce et al. [12], but a detailed account for how to actually design and build a modular tensegrity robotic system was out of the scope for that publication. In this section, we will go through each subsystem of the SUPERball and outline the structural and mechanical designs. A driving factor in the design of the SUPERball is the ability to replace a subsystem depending on changes to the system requirements. This allows for this single robotics system to be adaptable to changing parameters, such as different power requirements, actuation paradigms, spring constants, rod lengths, etc. Thus, the main subsystems are as follows: cable and spring, shaft collar, power, and actuation and rod end. These systems are labeled on an end-cap in figure 3. Since a rod will experience compression forces from cables and ground contacts, each subsystem needs to effectively transfer and/or withstand the maximum compression force listed in table I.

A. Cable and Spring Subsystem

A unique feature of SUPERball is its internal compression springs. Tensegrity systems require some form of compliance at the end of an actuated cable, and with many systems, either external extension springs are placed in line with stiff cabling or used compliant cabling [17] [18]. External extension springs are not ideal due to high likelihood that unwanted objects will get caught within the spring during locomotion. Compliant cabling is often highly non-linear in nature, e.g., parachute cord. This makes modeling dynamics difficult and induces undesired factors, such as cable creep and stretch memory. Pairing a stiff cable with a linear spring allows for the tensegrity robotic system to have passive compliance while keeping the spring-cable system as linear as possible. SUPERball places compression springs within the connecting tube of the structure to alleviate the entanglement issue. Thus, for an actuated cable in SUPERball, one end connects to the motor and spool on one endcap, and the other end is routed through another endcap in through the assembly and to the compression spring. Compression springs were chosen so that a known compression length could be achieved without worry of plastically deforming the spring. Using this design idead, a design challenge arises of how to route cabling to the springs.

Fig. 3.   SUPERball End-cap Assembly Subsystems.

In tensegrity systems, the ideal case is to place the cable attachments at the ends of the rods. In SUPERball, this leads to routing the cabling through all the subsystems. The solution developed is to encapsulate a simple Bowden cable running the internal length from rod end to beginning of the spring assembly. In the initial design phase of the SUPERball, a simple encapsulation method was used for ease of manufacturing.

Though the system worked in initial testing, it became apparent that the Bowden cable was insufficiently supported at the cables' exit point in the top assembly. The design had the cable's exit support built into the bottom spool cap, as shown in Figure 4. This did not account for the large forces in the required 90-degree bend before it exited the end-cap assembly, and so the outer cable sheath inevitably came unattached as these forces bent straining the inner braided cable. A redesign was needed such the inner cable did not deform when loaded against its exit point.

A fixture piece was designed that guided the cable out at a known orientation. The cable guide bracket shown in Figure 5 fits just underneath the top flaps of the upper sheet metal structure and is held in place by attachments to that structure on both the top and side flanges. The screw through the side sheet metal flange also doubles as the tightening screw for the clamp on the cable guide tube. By

Fig. 4.   Initial exit point for Bowden cable on SUPERball.

directing the cable out to the side of the inner support sheet metal brackets (adjacent to the various electronic control boards), it was allowed enough room to bend through a gentle angle down through the hole in the battery holder and through the rest of the assembly.

This crucial length of cable support, through the bending angle, is provided by a series of three overlapping plastic tubes. In order to reduce friction through the bend, the original housing is cut so as to stop near the exit of the battery holder, and
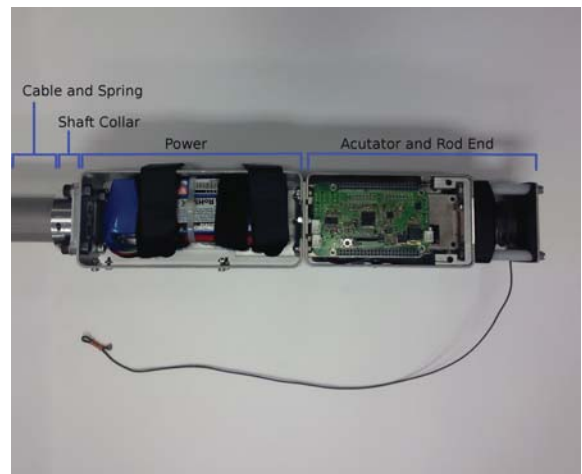
two concentric teflon tubes provide the cable guide for the remaining length. A thicker PETG tube is then press fit over these teflon tubes and the default cable sheath so as to secure the two sections of supports together.

The use of two overlapping tubes when exiting the cable guide bracket is motivated by the same desire for gentle bend radii outside the end-cap as inside. Having two steps of tube thicknesses outside the end-cap provides varying reaction forces against bends in the steel cable. Qualitative tests on SUPERball v1.0 showed that without an external, flexible support, the cable would permanently deform as it exited the end-cap just as badly as it would through harsh bends internal to the structure. During use, the cable will be pulled strongly at shallow angles once it has exited the end-cap. Using two stepped tubes helps reduce any pinch points, since each thickness will have a different bend radius when loaded. Figure 5 shows these two teflon tubes assembled into a brake cable guide bracket.

The bracket itself has also been optimized for manufacturing. With the notable exceptions of the thin slotting saw cut for the gap in the clamp, and the area removed by a Woodruff cutter that provides room for the head of the long 4mm bolt, this part can be made easily using a CNC mill.

B. Shaft Collar

A critical aspect of SUPERball is the ability to exchange end-caps relatively quickly. This is achieved by utilizing a simple shaft collar that clamps all the other subsystems to the connecting strut tube. Since this collar is the only mounting component of the end-cap, it needs to be robust to loading forces yet simple for easy assembly. The collar bolts onto both the battery compartment (and thereby the entire outer structure) as well as the internal cable-spring assembly. It then clamps onto the outside of the strut tube through a friction-based shaft collar connection. Figure 6(a) shows the first iteration of the shaft collar. This design worked well and met all of our design requirements, even though the design was over engineered with a safety factor magnitudes higher than our calculations dictated.

Fig. 5.   Cable Guide with teflon tubes inserted.
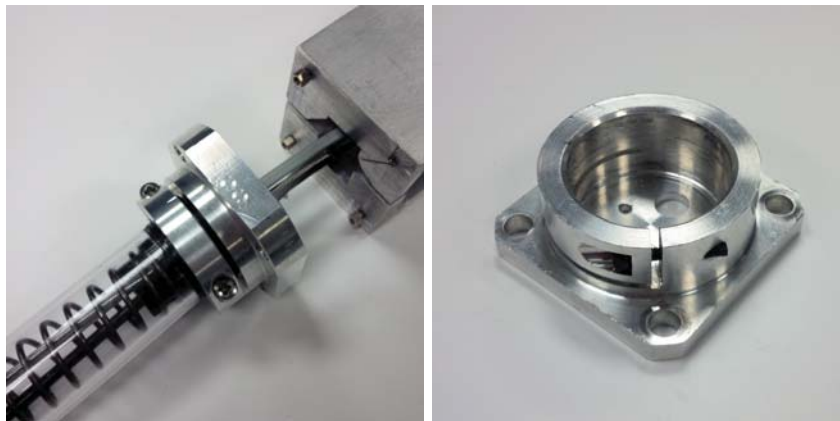
(a) Initial shaft collar for SUPERball. (b) Redesigned shaft collar for SUPERball.

Fig. 6.   Shaft Collar Iterations for SUPERball.

Upon making changes to the SUPERball, a new shaft collar was developed which focused on reducing mass and simplifying assembly even further. Three primary redesigns were executed on this part. First, the two-piece clamp design was changed to a single-piece, with only one screw. Removing the free piece reduces assembly difficulties, and eliminates a manufacturing step. Then, the overall weight of the piece was reduced significantly. Extensive finite element analysis work was performed (see section V) in order to optimize for weight reduction against safety factor. The final design retained the same basic geometry as the original, but with thinner walls.

C. Power Subsystem

The power subsystem consists of three main sets of components: a large lithium polymer battery, a controller PCB, and the sheet metal structure to which it is all attached.

As shown in Figure 7, initial design of this subsystem used two pieces of bulk aluminum milled out to house the battery. While this provided excellent structural support, multiple performance characteristics compelled a switch to a bent sheet metal aluminum design. First, weight was reduced significantly. After initial calculations indicated over-designed dimensions and an enormous safety factor for this part, these wall thicknesses were reduced to the point at which they effectively became sheet metal. Second, manufacturing became simpler: as opposed to a costly and complex CNC milling operation, this bracket could be cut from sheet with a water jet, then bent with a CNC sheet metal bender. Finally, more flexibility was required for placement of components.

Initial designs of placement of the large 3 Amp-hour battery compelled the need for dedicated tie-down straps, in order to facilitate exact placement of the component as well as allow for ease of replacing drained batteries. Thus, holes were needed for straps, shown in above pictures holding the battery to the side of the compartment.

In addition, systems-level design indicated the need for a discrete power management controller. A logical placement is physically close to the battery, which required more room than existed in the initial bulk design. The final version in Figure 7 shows multiple mounting holes for standoffs for such a printed circuit board, as well as slots for different straps to secure the battery as needed. It consists of five bends which fold together at the top section, and are then compressed together by the same bolt patter which attaches the compartment to the sheet metal surrounding the motor.

Sheet metal designs in the first iteration of SUPERball showed some microc-racks from harsh bending angles. Thus, this battery compartment was designed to account for gentler bend radii. Each of these bends was designed with a radius of three times the the sheet thickness, or 6mm. These same radii were used in the most recent version of the sheet metal brackets that support the motor and actuation subsystem.

Fig. 7. Left: Redesigned battery compartment. Right: Original battery compartment.

D. Actuation Subsystem

The actuation subsystem is designed for ease of assembly and manufacturing, as well as to further reduce friction in the motor-driven cable. Figure 8 displays the motor assembly, which at its core is similar to the one present on SUPERball's predecessor, ReCTeR. However, the new design is significantly more robust and versatile.

The simple, yet robust design of the cable actuator is based on a spindle actuated by a geared brushless DC motor. The motor axis is secured by two radial bearings, one of which is press fitted into the plate on top of the spindle and one is integrated into the gear box. A spindle (30mm diameter) machined out of POM sits on top of the motor axis and winds up a high strength flexible cable. More precisely, a 1.4mm Vectran cable (Cortland 7012 Vectran HT, Type 150) with a breaking strength of 2227N attaches to the spindle. Vectran cable has lower creep than Dyneema which was used on the previous prototype robot, but without protective coating it is sensitive to UV light [19], [20]. It has been successfully used in space applications (e.g., the Mars Pathfinder airbags) due to its excellent thermal properties.
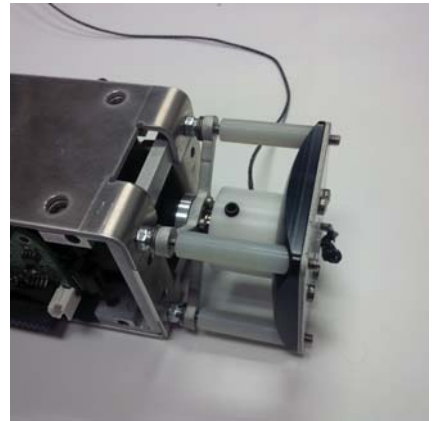

Fig. 8. Actuator design with bottom spool cap removed and exposed motor torque sensor. A POM spindle mounted onto the motor axis actuates a Vectran cable. This open construction exposes the wire and spindle, but reduces the cable friction and risk of knots. The design is shown without protective rubber cap.

The motor spindle has a guide passageway for the cable to pass through it, from the side to the top of the assembly (underneath any future protective rubber covering for the top). Therefore, the cable can slide into the spindle from the slide and come out on top of the assembly. This allows safe clamping of the cable without damaging it. We have studied various ways in which we can secure the one end of the Vectran cable that terminates underneath the rubber cap with minimal reduction of the breaking strength of the cable. The most promising option embeds a steel ball inside the cable and then pots that section of the cable in epoxy. Figure 10 shows this spindle with cable threaded through its guideway.

It is important to prevent tight bends (knots) of the cable, as this reduces its strength and increases wear. To further protect the cable and prevent it from getting stuck, the spindle is embedded into two smooth POM surfaces (spool caps), with a 0.5mm gap between the spindle and the surfaces. This allows the cable to slide smoothly in almost any direction without excessive friction.

In order for proper operation of the sensors attached to the motor torque mounting bracket, that component was not allowed to take any of the force from the rod end. The bottom spool cap is designed to take all the force from the upper components (nylon spacers and top plate, screwed on with one nut at the top) and transmit it directly to the motor sheet metal. The motor mount then floats freely in a small 1mm gap within a cavity in the bottom cap. Figure 9 shows a cross section of the end-cap in CAD, with the load patch highlighted. Note the flanges take the load from the nylon spacers, which are loaded from the top plate, instead of the motor mount piece itself. See the later Testing section for an analysis of the forces in these parts.

Fig. 9.   Path of compression load through actuation assembly.

This sensor on the cross-shaped motor mount is designed to measure the torque in the motor. Each actuated spring-cable assembly is effectively a series elastic actuator, because it attaches to a spring inside another bar. As such, it is in theory not needed to provided an elastic element on the motor mount. However, it is possible to replace this basic torque sensing element with a torsion spring design (e.g., as featured on the Robonaut [21] or the COMAN humanoid robot [22]). Another anticipated extension is a ratcheting mechanism to make it possible to mechanically disconnect the actuators from the spring-cable assemblies. This can be useful for drop tests or long-term stowage.

The assembly is powered by a 100W brushless DC motor (Maxon 386674, EC 22mm) reduced by a 109:1 gear box (Maxon 370784). As this is the first hardware iteration of SUPERball, we chose to optimize torque over speed. This gives us significant headroom to explore the robot's behavior with stiffer springs or under loading. More precisely, the current nominal output speed (cable retraction) is 0.42m/s with a cable tension of approximately 140N.

Fig. 10.   Spindle with Vectran cable.

Modularity is one of the interesting aspects of SUPERball and this is also reflected in the actuator and cable design. The initial build of SUPERball consists of 12 actuators which actuate half of the 24 outer shell tensile elements. One possible choice of actuation pattern is to fully actuate half of the 8 equilateral triangular faces of the robot (see Figure 3 in [12] and Figure 5 in [3]). However, some locomotion methods rely on the reduction of the ground contact area of the robot [16]. In this case, it might be sufficient to tighten a triangular face, instead of controlling its individual sides. In addition to this, we anticipate positioning a payload in the center of the robot. This can be realized by using 8 motors to control the tension of the 8 equilateral triangular faces, while the 4 remaining actuators position the payload. In practice, an outer shell cable would thus be actuated on one end-cap, then run along the two other end-caps on of the triangle and finally find its way into the first one, where it connects to an internal spring. This only requires a small redesign of the bolted-on cable guiding mechanism on a subset of the end-caps. Such clustered actuation mechanisms have already been considered in the static case [23], but to the best of our knowledge, no results are available about the dynamics of this actuation mechanism.

Finally, a rubber protective cap will be bolted onto the top of the end-cap. The optimal terrain friction coefficients have not yet been studied at this stage of the SUPERball project. As such, the protective cap has not yet been integrated into the physical design. Instead our current mechanical design seeks to obtain a sufficiently robust design without relying on the protective cap. The function of the rubber cap will thus initially be limited to additional protection against impact and scraping. In addition to this, the benefits of ground reaction force sensors for tensegrity control has not yet been established. It has thus not yet been decided if force transducers need to be embedded in the protective cap.
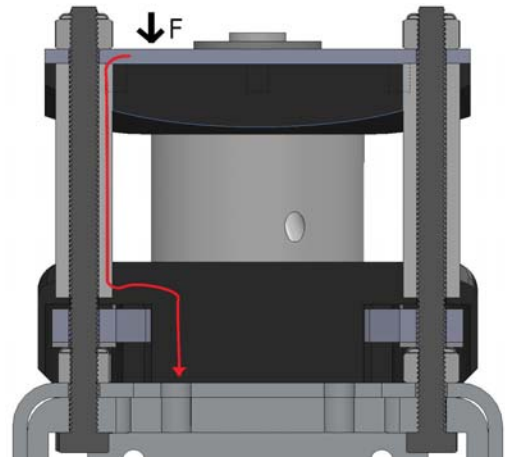
V. Hardware Testing

Different types of tests were performed on each of these designs of the end-cap, in accordance with the component's importance in relation to the overall design goals for SUPERball. In-depth testing was performed on subsystems whose failure modes were most severe, such as the structural subsystem. However, even if not discussed explicitly below, a minimum

of qualitative tests were performed for each part, to confirm a basic level of functionality. Future work will include more thorough testing and calibration for all components.

A. Structural System Testing

1) Analytical: The failure modes of the structural load-bearing elements in SUPERball are most severe, and were thus analyzed with a variety of techniques. First, analytical calculations were performed for failure modes of the structure, including the aluminum strut tube and sheet metal components. These calculations were performed in the initial design phase for components with simpler geometries; see below for numerical tests of complex parts.

For the strut tube, two basic calculations included tests for failure in axial loading as well as buckling. The force applied to the strut tube was calculated by assuming all eight cables attached to one rod applied the max load of 100N (from Table I), in line with the tube, for $F_a = 800N$. At the inner/outer diameter cited above for this design, axial stress is then

$$\sigma_a = \frac{F_a}{A} = \frac{800}{\frac{\pi}{4}(r_o^2 - r_i^2)} = \frac{800}{\frac{\pi}{4}((0.00331)^2 - (0.00349)^2)} = 8.4 \ MPa$$

This gives an axial compression failure safety factor of 32, using a yield strength of σ_f = 269 MPa for the 2024-T3 aluminum alloy from which this tube is made [24]. Similarly, using Euler's buckling approximation and a modulus of elasticity of $E = 73$ GPa,

$$F_{buckling} = \frac{\pi^2 EI}{(KL)^2} = \frac{\pi^2(73 * 10^9)(\frac{\pi}{64}(0.00349^4 - 0.00331^4))}{(2)(1)} = 2480 \ N$$

This gives a buckling failure safety factor of $2481/800 = 3.1$, which although small, is acceptable for this prototype. Additionally, a 3D stress state was calculated, assuming this axial load as well as hoop and shear stresses from a torsional load of the same magnitude. This last assumption was justified in the case of an incorrect tube placement: if the tube did not contact the face of the shaft collar, the entire $800N$ load would be transmitted through shear on the contact face. Assuming a coefficient of static friction of $\mu = 0.95$ for aluminum against aluminum [25], and a contact length of 10mm, the tube pressure, hoop stress, and shear stress were calculated to be

$$P_r = \frac{F_{pressure}}{A_{face}} = \frac{800/\mu}{2\pi rh} = \frac{800/0.95}{2\pi(0.0175)(0.01)} = 766 \ kPa$$

$$\sigma_h = \frac{P_r r}{t} = \frac{(766 * 10^3)(0.01657)}{8.89 * 10^{-4}} = 14.3 MPa$$

$$\tau_{yz} = \frac{F_{shear}}{A_{face}} = \frac{800}{2\pi rh} = \frac{800}{2\pi(0.0175)(0.01)} = 727 \ kPa$$

Note that in the above, the internal pressure on the thin-walled tube comes entirely from the clamping action of the shaft collar resisting the axial load. The von Mises stress from this calculation can then be compared to the yield stress of 2024-T3 aluminum. In SI units of MPa,

$$\boldsymbol{\sigma} = \begin{bmatrix} \sigma_h & \tau_{xz} & \tau_{xy} \\ \tau_{xz} & \sigma_a & \tau_{yz} \\ \tau_{xy} & \tau_{yz} & \sigma_r \end{bmatrix} = \begin{bmatrix} 14.3 & 0 & 0 \\ 0 & 8.4 & (0.727) \\ 0 & (0.727) & (0.766) \end{bmatrix}, \quad \sigma_{vm} = 11.82 \ MPa$$

This is larger than the original axial stress estimate, taking the compression failure safety factor down to $269/11.82 = 22$. From all this analysis, it is clear that the failure mode of the strut tube would be buckling, which currently has the small but acceptable safety factor of 3.

For the sheet metal brackets, a similar buckling analysis was performed. Here, similar properties of aluminum were used, with $\nu = 0.33$ [24]. Approximating each bent bracket as simply-supported, and assuming the bending process has not weakened the material significantly, the edge most likely to buckle is one long side of the battery compartment. This section that is 0.11m long with a cross-sectional area of 2mm by 60mm has a critical buckling force [26] of:

$$P_{cr} = \frac{\pi^2 EI}{(1 - \nu^2)a^2} = \frac{\pi^2(69 * 10^9)(\frac{1}{12}(0.06)(0.002)^3)}{(1 - (0.33)^2)(0.11)^2} = 2530N$$

Compared against a maximum worst-case load of $800N$ from above, this bracket has a safety factor against buckling of $2530/800 = 3.1$, which like the tube, is small but acceptable for a prototype.

2) Numerical: In addition to an analytical estimation of the factor of safety for parts with simpler geometries, finite element analysis tests were conducted for the other structural components. Specificallly, the end-cap shaft collar, battery compartment, and bottom spool cap were tested within Solidworks Simulation 2012. Each test was done as a compression test with the same worst-case load as estimated above of 800N.

The end-cap shaft collar test, shown in Figure 11, used the default material properties within Solidworks for 6061-T6 aluminum. The default mesh type was used, with a global element size of 1.75mm. The inner cylindrical face, where the collar clamps the strut tube, was constrained in all six degrees of freedom (fully built-in.) Then, a force of 800N was applied to the top face, where the battery compartment would attach. As expected, since this part was still relatively thick-walled, this test showed a maximum von Mises stress of only 7 MPa,

Fig. 11. FEA test of the end-cap shaft collar.

so this part had an estimated safety factor of 38 against the yield strength of 269 MPa. This indicated that the shaft collar piece was not a source of concern for failure.
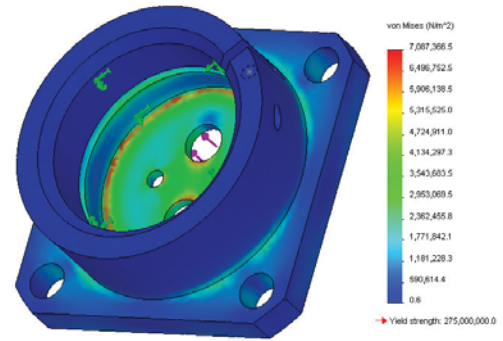
The static compression test of the battery compartment, shown in Figure 12, also used the default material properties within Solidworks for 6061-T6 aluminum. The default mesh type and size were also used. The bottom face, which contacts the end-cap shaft collar, was constrained in all six degrees of freedom. The topmost bent face, which bolts to the structural brackets surrounding the motor, had an applied normal load of 800N. Additionally, the Solidworks "Component Contact: Bonded" of

Fig. 12. FEA Test of the battery compartment.

two faces was applied between the three bent pieces of sheet metal at the top of the compartment that are compressed together when bolted. The test in Figure 12 shows a maximum von Mises stress of 135 MPa, leading to a safety factor of almost 2.

Fig. 13. FEA test of the bottom spool cap part.

This compares decently well with the simplistic stress calculation above, but does indicate that the initial simplistic calculations do not account for the bends in the sheet metal. Note that a bending test in FEA is not included in these results due to failures of the simulation to find a solution.

Two static compression tests of the bottom spool cap were also conducted, using the default material properties within Solidworks Simulation 2012 for Delrin acetyl resin, the raw material from which the part is made. The faces which contact the supporting sheet metal brackets were constrained in all six degrees of freedom. As before, the default mesh type and size were also used. Among the many forces this cap could experience, the compressive force on its inner flanges from the nylon spacers is expected to be most significant. As discussed above, these flanges transmit the entire load of impact of the rod end, as well as any loads from the radial bearing of the motor spindle. Two different tests were performed with loads of 100N and 800N. The former, shown
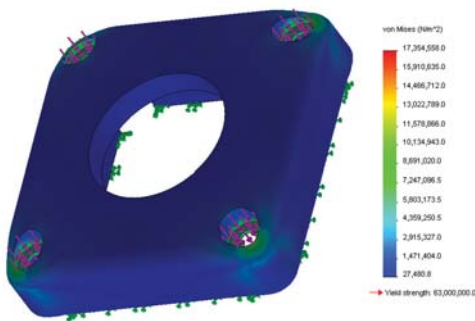
in Figure 13, was justified as a lower-end estimate of the force a rod would experience from its one actuated cable. For this smaller load, the maximum von Mises stress was 17 MPa, for a safety factor of 4.2 using the value of 72 MPa as the yield strength of Delrin [27]. However, the test with the larger load of 800N (worst case) showed a maximum von Mises stress of 133 MPa, which was a factor of 8 larger than the other test as expected. This larger value would cause failure in the part, and thus helped identify this as a potential failure mode and candidate for future redesign.

(a) Compression test setup for end-cap prototype.

(b) Bending test setup for end-cap prototype.

Fig. 14. Low-fidelity experimental test of prototype of modular end-cap assembly.

3) Experimental: A final set of experimental tests were conducted with a full prototype of the end-cap assembly. First, tests in compression and bending were performed, in order to validate various conclusions of the analytical and FEA tests. Finally, a short drop test was performed that sought to mimic some of the conditions this robot might experience in the future when used as a planetary rover. Note that none of the tests were performed until failure of the sheet metal, since practical considerations required re-use of these specific components.

An assembled end-cap, in its rig for the compression test, is shown in Figure 14(a). This low-fidelity test placed the end-cap, in series with a scale, between a hydraulic jack and a fixed support. Increasing force from the jack up to approximately 1000N, just over the worst-case estimate of 800N. For the sheet metal brackets and end-cap, no plastic deformation or failure was detected during this test, indicating that the assembly would survive such forces. However, as shown in Figure 15, the bottom spool cap flanges did indeed shear off as suggested by the FEA test. Thus, a future redesign of these flanges would be required if such large forces were to be applied in practice.
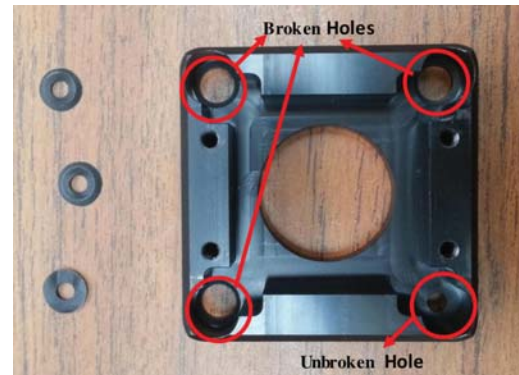

Fig. 15. Results from compression test. Flanges on bottom spool cap have sheared, confirming the factor-of-safety predicted by the FEA results.

Similarly, Figure 14(b) shows a test of a bending moment on the end-cap. Although no such force is expected to be applied to the structure, and was not designed for, this test was performed as a precaution against unexpected situations during locomotion testing of this prototype. The end-cap was horizontally clamped to a fixture, and then the scale was again placed in series with the hydraulic jack, which was used to apply a force of $54N$ to the rod end section of the end-cap. Again, no failure of any type was detected during tests, indicating that the assembly's robustness to unintentional collisions or loads.

Finally, a short drop test was performed using a fishing line as a guide for the end-cap and strut assembly to hit the ground at a specified angle. The left of Figure 16 shows the test setup. A piece of fishing line was attached to a fixture roughly 20 feet above a dirt and gravel bed, and then fixed into place in the ground at a net angle of roughly 60 degrees. This height of about 20 feet corresponds to one-fifth the total energy with which a SUPERball would collide with the surface of Titan, Saturn's moon [1]. Then, the end-cap assembly, attached to a strut tube, was placed on this fishing line and dropped. The right image of Figure 16 shows the results of this drop test: the flanges in the bottom spool cap, previous identified as a potential location of failure, did indeed shear apart upon impact. In this case, the nylon spacers forced the flanges apart from the cap body, and are lodged into the space below the cap. Additionally, one long stainless steel M4 screw (inside

the nylon spacer) deformed slightly. This test identified areas of improvement for future revisions that would be hardened against larger drop tests: the sheet metal aluminum structure performed as expected, but the Delrin part and thin M4 bolt should be redesigned.

Fig. 16. Results of drop test. Left: End-cap and rod impact the ground. Right: Close-up of end-cap actuation area after impact, where the flanges on bottom spool cap have again sheared as the nylon spacers push through. Note that these forces are much greater than those expected under locomotion.

All of these tests showed the basic validity of the structure used for SUPERball. Although a more thorough confirmation of results would include tests until failure for metal parts, as well as a wider variety of tests, these were sufficient for the purposes of this prototype. These structural tests show that this robot is unlikely to break during its locomotion tests, and that the operators are likely safe when performing such dynamic tests.

B. Other testing

For the strain gauges and sensors, simple qualitative tests were peformed to verify that sensor output responded to deflections along the desired axes. The strain gauge component in the Cable-and-Spring assembly responded well when compressed axially, and the motor mount torque sensor did so when put under torsion. A data collection and calibration mechanism for the sensors is currently under development for more thorough verification.

VI. Future Work

This work describes first steps in validating the structural design of our first modular tensegrity end-caps intended for use on the SUPERball robot. Now that the design of the end-caps is finalizing, our next steps will be to build twelve of the end-caps described here and build a full new version of the SUPERball robot. This prototype will be used primarily for controls and locomotion testing across a range of challenging terrains, and will provide an opportunity to port control concepts developed in the NTRT simulator to actual hardware.

As the completed robot will be used in locomotion and mobility tests, forces internal to the structure are to be calculated and compared against predicted values. Since the engineering requirements for this structure were derived from a control algorithm within simulation, it is expected that there will be some variance from the desired 100N maximum. Measuring and quantifying such metrics will allow for better design in future revisions.

After the locomotion testing, we will continue work on the design of our second end-cap which will focus on two key design criteria: the ability to actuate two cables from each end-cap, and the mechanical robustness to survive a 15 m/s landing, which is the expected terminal-velocity of SUPERball landing on the moon Titan. While building up our "family" of modular end-caps, we also intend to develop smaller, lighter end-caps which would be appropriate for use in our related research into spine-like tensegrity robots.

It is the authors' hope that these designs help others in the construction of robust tensegrity robots for extended locomotion tests, and that this work contributes to the overall goal of designing tensegrity robots for unique, dynamic locomotion.

VII. Acknowledgments

REFERENCES

[1] V. SunSpiral, G. Gorospe, J. Bruce, A. Iscen, G. Korbel, S. Milam, A. Agogino, and D. Atkinson, "Tensegrity based probes for planetary exploration: Entry, descent and landing (EDL) and surface mobility analysis." *To Appear in International Journal of Planetary Probes*, July 2013.

[2] D. E. Ingber, "Tensegrity I. Cell structure and hierarchical systems biology," *Journal of Cell Science*, vol. 116, no. 7, pp. 1157–1173, 2003.

[3] Y. Koizumi, M. Shibata, and S. Hirai, "Rolling tensegrity driven by pneumatic soft actuators," in *IEEE International Conference on Robotics and Automation (ICRA)*, 2012, pp. 1988–1993.

[4] J. M. Mirats-Tur and J. Camps, "A three-dof actuated robot," *Robotics & Automation Magazine, IEEE*, vol. 18, no. 3, pp. 96–103, 2011.

[5] J. M. Mirats-Tur, "On the Movement of Tensegrity Structures," *International Journal of Space Structures*, vol. 25, no. 1, pp. 1–14, 2010.

[6] V. A. Webster, A. J. Lonsberry, A. D. Horchler, K. M. Shaw, H. J. Chiel, and R. D. Quinn, "A segmental mobile robot with active tensegrity bending and noise-driven oscillators," in *IEEE/ASME International Conference on Advanced Intelligent Mechatronics (AIM)*. IEEE, 2013, pp. 1373–1380.

[7] M. Khazanov, B. Humphreys, W. Keat, and J. Rieffel, "Exploiting dynamical complexity in a physical tensegrity robot to achieve locomotion," in *Advances in Artificial Life, ECAL*, vol. 12, 2013, pp. 965–972.

[8] V. Bohm and K. Zimmermann, "Vibration-driven mobile robots based on single actuated tensegrity structures," in *IEEE International Conference on Robotics and Automation (ICRA)*. IEEE, 2013, pp. 5475–5480.

[9] J. Rieffel, R. Stuk, F. Valero-Cuevas, and H. Lipson, "Locomotion of a tensegrity robot via dynamically coupled modules," *Proceedings of the International Conference on Morphological Computation*, 2007.

[10] J. Rieffel, B. Trimmer, and H. Lipson, "Mechanism as mind: What tensegrities and caterpillars can teach us about soft robotics," in *Proceedings of Artificial Life XI*, 2008, pp. 506–512.

[11] J. Rieffel, F. J. Valero-Cuevas, and H. Lipson, "Morphological communication: exploiting coupled dynamics in a complex mechanical structure to achieve locomotion." *Journal of the Royal Society Interface*, vol. 7, no. 45, pp. 613–21, Apr. 2010.

[12] J. Bruce, K. Caluwaerts, A. Iscen, A. P. Sabelhaus, and V. SunSpiral, "Design and evolution of a modular tensegrity robot platform," in *IEEE International Conference on Robotics and Automation (ICRA)*, 2014.

[13] J. Bruce, A. Sabelhaus, Y. Chen, D. Lu, K. Morse, S. Milam, K. Caluwaerts, A. Agogino, and V. SunSpiral, "SUPERball: Exploring tensegrities for planetary probes," in *12th International Symposium on Artificial Intelligence, Robotics and Automation in Space (i-SAIRAS)*, 2014.

[14] B. Mirletz, I. W. Park, T. E. Flemons, A. K. Agogino, R. D. Quinn, and V. SunSpiral, "Design and control of modular spine-like tensegrity structures," in *The 6th World Conference of the International Association for Structural Control and Monitoring (6WCSCM)*, 2014.

[15] BulletPhysicsEngine, "http://www.bulletphysics.org/," 2013.

[16] K. Caluwaerts, J. Despraz, A. Iscen, J. Bruce, A. P. Sabelhaus, B. Schrauwen, and V. SunSpiral, "Design and control of compliant tensegrity robots through simulation and hardware validation," *Submitted*, 2014.

[17] J. Rieffel, R. J. Stuk, F. J. Valero-Cuevas, and H. Lipson, "Locomotion of a tensegrity robot via dynamically coupled modules," in *Proceedings of the International Conference on Morphological Computation*, 2007.

[18] M. Shibata and S. Hirai, "Rolling locomotion of deformable tensegrity structure," in *12th International conference on climbing and walking robots and the support technologies for mobile machines*, 2009, pp. 479–486.

[19] R. B. Fette and M. F. Sovinski, "Vectran fiber time dependant behavior and additional static loading properties," DTIC Document, Tech. Rep., 2004.

[20] M. Said, B. Dingwall, A. Gupta, A. Seyam, G. Mock, and T. Theyson, "Investigation of ultra violet (UV) resistance for high strength fibers," *Advances in Space Research*, vol. 37, no. 11, pp. 2052–2058, 2006.

[21] M. A. Diftler, J. Mehling, M. E. Abdallah, N. A. Radford, L. B. Bridgwater, A. M. Sanders, R. S. Askew, D. M. Linn, J. D. Yamokoski, F. Permenter, *et al.*, "Robonaut 2-the first humanoid robot in space," in *IEEE International Conference on Robotics and Automation (ICRA)*, 2011, pp. 2178–2183.

[22] N. G. Tsagarakis, M. Laffranchi, B. Vanderborght, and D. G. Caldwell, "A compact soft actuator unit for small scale human friendly robots," in *IEEE International Conference on Robotics and Automation (ICRA)*, 2009, pp. 4356–4362.

[23] K. Moored and H. Bart-Smith, "Investigation of clustered actuation in tensegrity structures," *International Journal of Solids and Structures*, vol. 46, no. 17, pp. 3272–3281, 2009.

[24] MatWeb Materials Property Data, "Aluminum 2024-t3," 2014. [Online]. Available: http://www.matweb.com/search/DataSheet.aspx?MatGUID=57483b4d782940faaf12964a1821fb61&ckck=1

[25] The Engineering Toolbox, "Friction coefficients," 2014. [Online]. Available: http://www.engineeringtoolbox.com/friction-coefficients-d_778.html

[26] D. W. A. Rees, *Appendix C: Plate Buckling Under Biaxial Compression and Shear*. John Wiley and Sons, Ltd, 2009, pp. 537–541. [Online]. Available: http://dx.doi.org/10.1002/9780470749784.app3

[27] DuPont Plastics, "Delrin design information," 2014. [Online]. Available: http://www2.dupont.com/Plastics/en_US/assets/downloads/design/DELDGe.pdf